Acta Oceanol. Sin., 2019, Vol. 38, No. 11, P. 40–50
https://doi.org/10.1007/s13131-019-1497-0
http://www.hyxb.org.cn
E-mail: hyxbe@263.net

A numerical study on salinity stratification at the Oujiang River Estuary, China

Yichun Li[1], Jingui Liu[2]*

[1] College of Civil Engineering and Architecture, Beibu Gulf University, Qinzhou 535011, China

[2] Key Laboratory of Research on Marine Hazards Forecasting, National Marine Environmental Forecasting Center, Beijing 100081, China

Received 17 September 2018; accepted 29 October 2018

Abstract

The Oujiang River Estuary (ORE) is a macrotidal estuary with drastic variation of river discharge and large tidal range. Numerical simulations based on the unstructured grid, Finite-Volume, primitive equation Community Ocean Model (FVCOM) are conducted to investigate the intratidal and intertidal variations of salinity with an extremely upstream river boundary and large computational domain. The dynamic equation of potential energy anomaly is adopted to evaluate the stratification and mixing processes from model results. Meanwhile, the stability of estuarine stratification on different timescales and its spatial variation are studied using estuarine Richardson number and stratification parameter. The critical values of tidal range and river discharge that determine the stratification state are obtained. The critical values exhibit distinct spatial difference. The north branch of the ORE exhibits well-mixed conditions when the tidal range exceeds 3.8, 4.0 and 4.6 m at upper inlet, middle segment and the river mouth, respectively. When river discharge is below 280 m^3/s or exceeds 510 m^3/s, the upper part of the north branch is well-mixed sustainably. Near the river mouth, river discharge of 280 m^3/s is a rough critical value that separates well-mixed and stratified states. It is also concluded that periodic stratification exists in the North Channel. The lower estuary appears to be partially stratified at early ebb or early flood tide, and well-mixed in other tidal stages. The stratification only develops during early ebb in the upper segment. The enhancement of stratification is mainly caused by longitudinal advection and lateral velocity shear, while turbulent mixing and longitudinal tidal strain are the main factors of stratification attenuation.

Key words: stratification, the Oujiang River Estuary, FVCOM, Macrotidal Estuary, potential energy anomaly

Citation: Li Yichun, Liu Jingui. 2019. A numerical study on salinity stratification at the Oujiang River Estuary, China. Acta Oceanologica Sinica, 38(11): 40–50, doi: 10.1007/s13131-019-1497-0

1 Introduction

Estuarine stratification plays an important role in estuarine processes, such as vertical gravitational circulation, estuarine secondary circulation, sediment transport, classification of the estuary, etc. (Monismith et al., 1996; Cheng et al., 2009; Lin et al., 2012; Flores et al., 2017). To quantify estuarine stratification, several metrics are suggested, such as stratification number, estuarine Richardson number, gradient Richardson number, Froude number et al. (Dyer, 1997; Fischer, 1972). A widely used metric is potential energy anomaly proposed by Simpson (Simpson and Bowers, 1981; Simpson et al., 1990). Simpson et al. (1991) and Bowers provided a series of metrics of stratification generation and extinction relating to sea surface heat, bottom friction and tidal mixing. This method has recently been applied in many estuarine studies (Ralston et al., 2013; Marques et al., 2011; de Vries et al., 2015; Pu et al., 2015). Burchard and Hofmeister (2008) proposed a dynamic equation for potential energy anomaly, and de Boer and Pietrzak et al. (2008) also derived a similar equation simultaneously. In most estuaries and coastal waters, riverine buoyancy results in vertical density variation that increases stratification, while tidal mixing decreases stratification and causes the water density to be more uniformly distributed in vertical. Generally, enhanced mixing during flood destabilizes the stratification of the water column, accompanied with the tidal flow pushing the fresh water back to the upstream. On the other hand, tidal straining and weak mixing make the estuary well-stratified during ebb (Chant and Stoner, 2001; Burchard and Hofmeister, 2008). Tidal straining is the effect of vertically sheared velocity acting on the horizontal density gradient. It results in stratification asymmetry during tidal cycles. This paper tries to analyze the relevant terms of stratification and mixing processes from model results, thus qualify the terms relevant for generation and destruction of stratification using the dynamic equation for the potential energy anomaly.

Estuaries may be classified into different types according to different vertical structures of salinity and hydrodynamic behaviors (Dyer, 1997; Valle-Levinson, 2010). Due to different time scales of the variation of river discharge and tidal range, stratification may exhibit significant temporal changes. Stratification exists during some periods and disappears during other times in a tidal cycle (Sharples et al., 1994). Meanwhile, as the variation of tidal, riverine dynamics and bathymetry along and across the river, stratification also shows significant spatial changes. Temporal and spatial variations of estuarine stratification affect vertical mixing and suspended materials transport.

There are different methods in estuarine classification (Dyer,

Foundation item: The National Key Research and Development Program of China under contract No. 2016YFC1401802.
*Corresponding author, E-mail: lehel1104@yahoo.com

1997; Valle-Levinson, 2010), based on either one parameter or two parameters. The Oujiang River Estuary (ORE) is located in the Zhejiang Province, China (Fig. 1). River discharge ranges from dozens of m^3/s to more than 8 000 m^3/s. The maximum tidal range can reach 8 m. In the ORE, previous studies are mainly in regard to reclamation engineering (Wang and Li, 2001; Wang and Shen, 2014; Xu and You, 2016). In recent years, fundamental research has been emphasized substantially (Lin et al., 2012; Xu and You, 2017). However, there were still few research about the classification and stratification in the ORE. In the coastal engineering field, according to general understanding, the ORE is roughly considered as well-mixed since its large tidal range. It is evidently oversimplified. Lin et al. (2012) studied the estuarine type of the ORE using the Hansen and Rattary method and estuarine Richardson number. However, only some averaged values of rive discharge and tidal range were used. They also did not consider the spatial and temporal variations of the estuarine type of the ORE. Thus variations of stratification and estuarine classification on different timescales are analyzed on the base of numerical simulations forced by real discharges and tidal range. Besides, previous researchers defined the riverine boundary not more upstream than Maiao where is significantly affected by tide. Meanwhile, the sea boundary is not far enough for such a complicated area where many islands are located outside the ORE mouth. In this paper, numerical simulations are performed in the ORE with a specified upstream boundary at Weiren where only river flow works. Variation of stratification is analyzed on intra- and inter-tidal time scales, and stratification mechanisms are investigated based on dynamic equation of potential energy anomaly. The structure of this paper is organized as follows: In Section 2, the study area is described. The establishment and validation of the numerical model come in Section 3. Subsequently, the results, stratification mechanics and classification of the ORE are discussed in Section 4. Finally, conclusions are presented in Section 5.

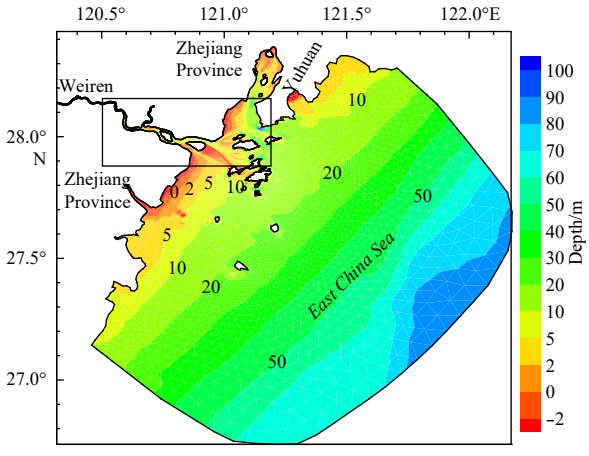

Fig. 1. Topography and model domain in the Oujiang River Estuary.

2 Study area

The Oujiang River, which passes through the Wenzhou City, originates from the mountains in western Zhejiang Province and empties into the East China Sea. Numerous islands exist along the river mouth and nearshore areas. Among them, there are three islands in this river, i.e., Jiangxinyu Island, Qidu Island and Lingkun Island. The most upstream one is Jiangxinyu Island, which bounds Wenzhou City to the north. In the middle, Qidu Island divides the river into two sub-channels, which have almost equivalent water fluxes. The north channel has a maximum depth of about 20 m and is slightly narrower than the south channel with a maximum depth of about 16 m. The Lingkun Island near the river mouth is the largest island. The north branch is the main waterway of the ORE with a main channel near the concave bank. The south branch is very shallow and not inundated during low tidal phase. Diversion rate of the two branches is about 7:3. A submerged dike was constructed several decades ago at the upper inlet of the south branch. Immediately upstream of the submerged dike, a hollow with a maximum depth of about 33 m is located near the south bank. Outside the river mouth, many islands of different scale scatter over the nearshore zone, e.g., Damen Island, Xiaomen Island and Niyu Island. Semi-closed Yueqing Sound is located to the north of the river mouth. The Lingkun Island and The Niyu Island are connected by embankments to promote hydraulic fill. Three waterways to different directions are separated by the Damen and Xiaomen Islands.

The Nanxijiang River is the largest tributary along the ORE. A hydrological station Weiren (WR) upstream provides long-term discharge measurements of the main branch. The multi-year averaged riverine discharge is about 470 m^3/s. The maximum value during flood can be more than 8 000 m^3/s. The ORE is a marcotidal estuary where the M_2 constituent dominates with a tidal range of approximately 6 m during spring tide. The largest velocity of tidal current in the north branch can reach upwards of 2 m/s. The tidal limit and salinity water limit are around Weiren and Qidu Islands, respectively. Under ordinary river discharge, the salinity in the lower estuary varies significantly at different tidal phases due to its short length and strong tide.

3 Numerical model

3.1 *Model description*

The unstructured-grid Finite Volume Coastal Ocean Model, i.e., FVCOM (Chen et al., 2003), is a widely used model in estuarine studies. Due to its capability in fitting complex land boundaries, FVCOM is adopted to simulate the hydrodynamics processes in the ORE. The upstream boundary of the main tributary is set at Weiren (WR) with daily runoff. The open sea boundary extends to about 100 and 70 km in the alongshore and offshore directions, respectively. The tidal forcing at the open boundary is predicted using the NAOTIDE database. The mesh grid ranges from about 30 m in the river to about 9 km near the sea boundary. 20 sigma-layers are evenly set in the vertical direction. The salinity values are set to 0 and 35 at the upstream and sea boundaries, respectively. Time step of inner mode is 0.1 s. *k-kl* turbulence model with the wall function modified as that proposed by Burchard and Baumert (Burchard and Baumert, 1998; Warner et al., 2005) is adopted. Wind stress is not imposed in this study since it is not significant during the field measurement periods. The numerical simulations are started from the rest state and run 40 d before the field observation period and then continue to a 60 d duration to include the freshet around July 20, 2005. The velocity data in the river are decomposed to the along-stream and cross-stream components, defined as the direction of maximum and minimum variance of the depth-averaged horizontal velocity vector (de Vries et al., 2015).

3.2 *Stratification equation*

The results from numerical simulations are investigated to analysis the stratification mechanics in the ORE. The dynamic

equation of potential energy anomaly proposed by Burchard and Hofmeister (2008) is adopted, which can be rewritten as:

$$\begin{aligned}\frac{\partial \phi}{\partial t}=&-\frac{\partial}{\partial x}\left(\bar{u}\phi\right)-\frac{\partial}{\partial y}\left(\bar{v}\phi\right)+\frac{g}{D}\frac{\partial \bar{\rho}}{\partial x}\int_{-H}^{\eta}z\tilde{u}\mathrm{d}z+\frac{g}{D}\frac{\partial \bar{\rho}}{\partial y}\times\\&\int_{-H}^{\eta}z\tilde{v}\mathrm{d}z+\frac{\rho_0}{D}\int_{-H}^{\eta}P_{\mathrm{b}}\mathrm{d}z-\frac{g}{D}\int_{-H}^{\eta}\left(\eta-\frac{D}{2}-z\right)\tilde{u}\frac{\partial \tilde{\rho}}{\partial x}\mathrm{d}z-\\&\frac{g}{D}\int_{-H}^{\eta}\left(\eta-\frac{D}{2}-z\right)\tilde{v}\frac{\partial \tilde{\rho}}{\partial y}\mathrm{d}z-\frac{g}{D}\int_{-H}^{\eta}\left(\eta-\frac{D}{2}-z\right)\times\\&\tilde{w}\frac{\partial}{\tilde{\rho}}\partial z\mathrm{d}z-\frac{\rho_0}{2}\left(P_{\mathrm{b}}^{\mathrm{s}}+P_{\mathrm{b}}^{\mathrm{b}}\right)+\frac{g}{D}\int_{-H}^{\eta}\left(\eta-\frac{D}{2}-z\right)Q\mathrm{d}z+\\&\frac{g}{D}\int_{-H}^{\eta}\left(\eta-\frac{D}{2}-z\right)\nabla_{\mathrm{h}}\left(K_{\mathrm{h}}\nabla_{\mathrm{h}}\rho\right)\mathrm{d}z,\end{aligned}\tag{1}$$

where ϕ, u, η and H are potential energy anomaly, horizontal velocity, water level and water depth, respectively. ρ_0 and $\bar{\rho}$ are reference density and vertically averaged density, respectively. $\tilde{\rho}=\rho-\bar{\rho}$. $\tilde{\omega}=\omega-\bar{\omega}$, where ω and $\bar{\omega}$ are vertical velocity and a deduced vertical velocity of linear distribution respectively. K_{h} is horizontal eddy diffusivity. P_{b} is vertical buoyancy flux, and the superscripts s and b mean surface and bottom. D is total water depth. On the right-hand side, $\frac{\partial}{\partial x}\left(\bar{u}\phi\right)$ and $\frac{\partial}{\partial y}\left(\bar{v}\phi\right)$ are advection due to vertical mean horizontal along- and cross-stream velocity. $\frac{g}{D}\frac{\partial \bar{\rho}}{\partial x}\int_{-H}^{\eta}z\tilde{u}\mathrm{d}z$ and $\frac{g}{D}\frac{\partial \bar{\rho}}{\partial y}\int_{-H}^{\eta}z\tilde{v}\mathrm{d}z$ present depth-mean straining due to the vertical mean horizontal density gradient strained by the deviation from vertical mean velocity. $\frac{\rho_0}{D}\int_{-H}^{\eta}P_{\mathrm{b}}\mathrm{d}z$ is vertical mixing. $\frac{g}{D}\int_{-H}^{\eta}\left(\eta-\frac{D}{2}-z\right)\tilde{u}\frac{\partial \tilde{\rho}}{\partial x}\mathrm{d}z$ and $-\frac{g}{D}\int_{-H}^{\eta}\left(\eta-\frac{D}{2}-z\right)\tilde{v}\frac{\partial \tilde{\rho}}{\partial y}\mathrm{d}z$ are non-mean straining. $\frac{g}{D}\int_{-H}^{\eta}\left(\eta-\frac{D}{2}-z\right)\tilde{w}\frac{\partial \tilde{\rho}}{\partial z}\mathrm{d}z$ present vertical advection. $\frac{\rho_0}{2}\left(P_{\mathrm{b}}^{\mathrm{s}}+P_{\mathrm{b}}^{\mathrm{b}}\right)$ and $\frac{g}{D}\int_{-H}^{\eta}\left(\eta-\frac{D}{2}-z\right)Q\mathrm{d}z$ are surface and bottom buoyancy fluxes and inner sinks or sources of potential density respectively. $\frac{g}{D}\int_{-H}^{\eta}\left(\eta-\frac{D}{2}-z\right)\nabla_{\mathrm{h}}\left(K_{\mathrm{h}}\nabla_{\mathrm{h}}\rho\right)\mathrm{d}z$ means the variations due to horizontal turbulent transport.

Three sample points set in the north branch (Fig. 1) are used to calculate the individual terms in Eq. (1) numerically. Since the water density in estuarine area is more affected by salinity than temperature which is different to that in far offshore areas where the density is significantly influenced by temperature. The water density is calculated using the state equation with temperature neglected (MacCready and Geyer, 2010; Geyer and MacCready, 2014):

$$\rho=\rho_0\left(1+\beta S\right),\tag{2}$$

where $\beta\simeq 7.7\times10^{-4}$, S is salinity.

3.3 *Model validation*

The field data of tidal level, velocity and salinity are collected (Shanghai Marine Engineering Survey and Design Institute (SMESD), 2005). Hourly tidal level data is from June 20 to July 4, 2005 at six stations. Tidal currents are during June 26–27, 2005. These data are rearranged to be 25 h-long series with one-hour interval. The tidal currents are at six depth layers vertically: surface, 0.2D, 0.4D, 0.6D, 0.8D and bottom. The surface and the bottom layer velocity is measured at the 0.5 m below sea surface and above the bottom, respectively. Sampling intervals and measurement depths of salinity are the same as tidal velocity.

Figure 3 shows the river discharges of WR and the Nanxi River. Figures 4–6 indicate the comparisons between observed and modeled data of tidal level, velocity and salinity. The negative and positive values represent flood tide and ebb tide, which depend on current direction. Most modeled results show acceptable agreements with observations. Additionally, three indices are used to quantify the agreements. A skill that has been widely used is written as the follows (Willmott, 1981; Li et al., 2005):

$$Skill=1-\frac{\sum_{i=0}^{n}\left|x_{oi}-x_{mi}\right|^2}{\sum_{i=0}^{n}\left(\left|x_{oi}-\overline{x_{o}}\right|+\left|x_{mi}-\overline{x_{o}}\right|\right)^2},\tag{3}$$

where the subscripts o and m indicate observed and modelled values, respectively, n is the number of samples. Another index used here to evaluate the absolute deviation of velocity and salinity is MAE (Mayer and Butler, 1993):

$$MAE=\frac{\sum\left|x_{oi}-x_{mi}\right|}{n}.\tag{4}$$

The deviation of current direction is collected using MAEA defined in Eq. (5). Comparing to Eq. (4), the Eq. (5) emphasizes the contributions in the main directions and weakens the influences arose from the slow slack flow that might be measured less precisely. The weights are chosen as square velocity amplitudes in the sense of kinetic energy.

$$MAEA=\frac{\sum_{i=0}^{n}\left(x_{oi}-x_{mi}\right)u_i^2}{\sum_{i=0}^{n}u_i^2},\tag{5}$$

where u is velocity, others are the same as defined above.

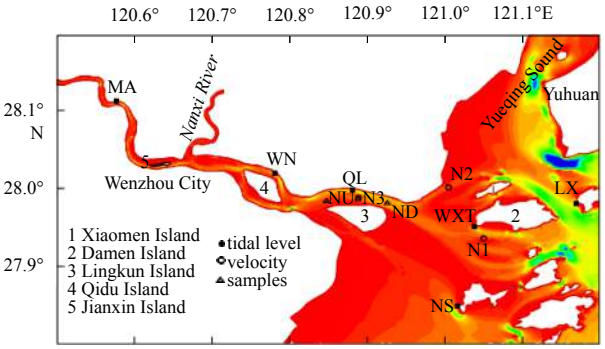

Fig. 2. Local topography corresponding to the square in Fig. 1 and data locations. Square marks tidal level, circle shows the site of observed velocity, and samples indicate the nodes where model results are investigated. Numbers 1–5 indicates the five main islands. MA represents Meiao, WN Wuniu, QL Qili, WXT Wuxiantou, LX Luxi.

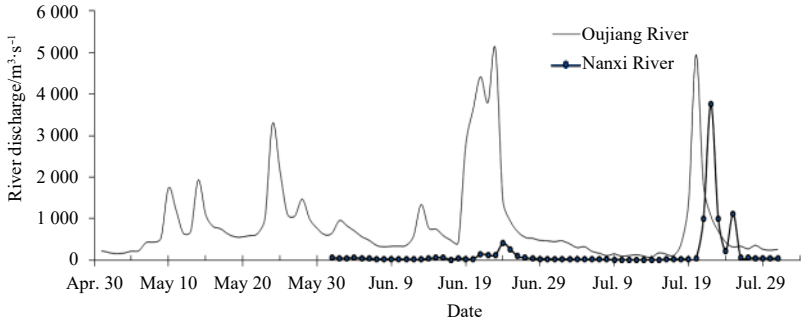

Fig. 3. River discharges of Oujiang River and Nanxi River. Real line is of Oujiang River while dotted line for Nanxi branch.

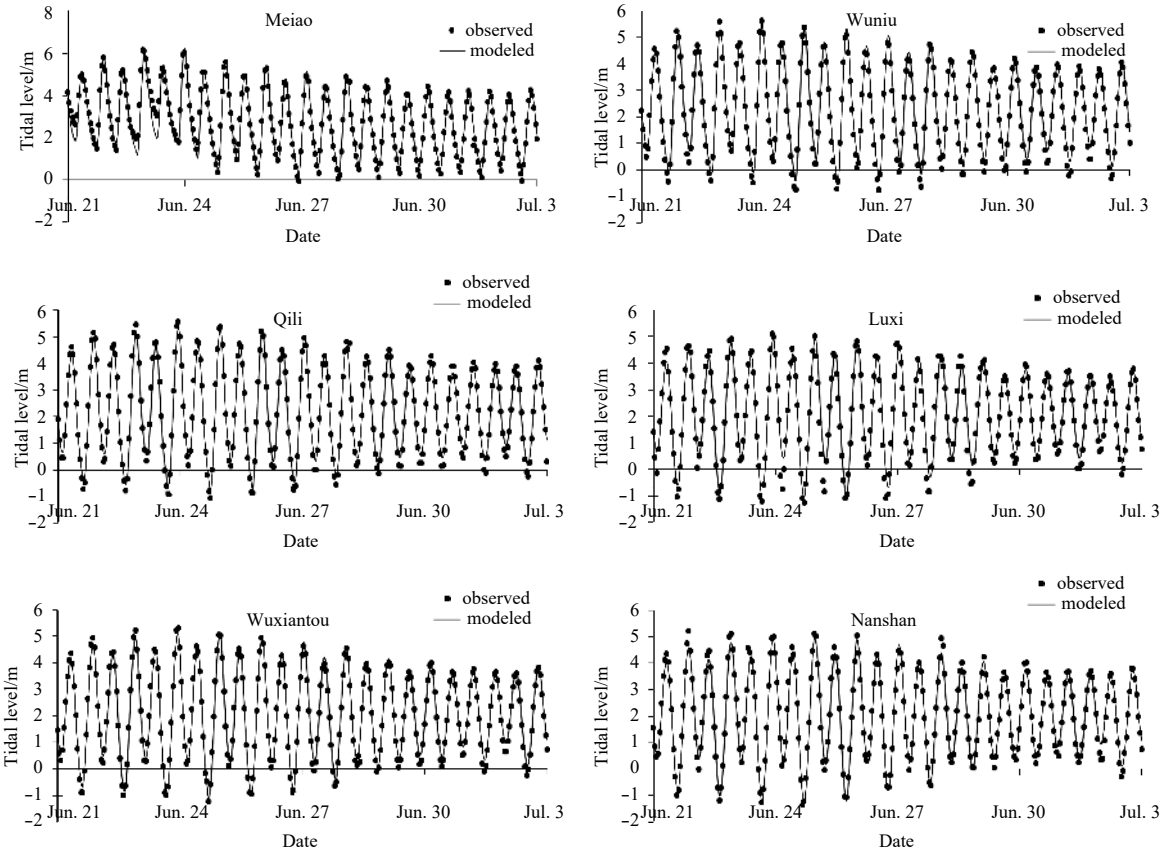

Fig. 4. Comparisons of tidal level.

The statistics of tidal level, velocity and salinity are listed in Table 1 and Table 2. For tidal level, the MAEs vary from 0.19 to 0.3 m. Compared to the tidal ranges of about 6 m, these deviations are acceptable. The index Skills are all larger than 0.97. MAEs of velocity are between 0.15 and 0.29 m/s. Deviations of the bottom layers are less than those of surface layers. The modeled and observed data are not measured at exactly the same depth, and this influence combined with grid resolution might produce some large deviations. However, the relatively large Skills show acceptable performance. MAEAs of current direction calculated using Eq. (5) are less than 16°. Skills of current direction are all lager than 0.9. MAEs of salinity are less than 3 except for N1 at surface layer. Large deviation at N1 may be caused by the relatively low measured values at early stage of measure period due to episodic events. The skills of salinity are all more than 0.8. According to the above analyses, the modeled results are conducted as acceptable.

4 Results and discussion

Three points NU, N3 and ND (Fig. 2) are chosen for the analyses of stratification, which are located at the center of the north branch. The ND is at the mouth, the N3 represents the middle part of the north branch, and the NU is located near the conjunction in the upstream inlet of the north branch. Upstream the NU, the water is quite fresh during most of the tidal stages. The stratification mechanism is analyzed based on the Eq. (1) at each point. Then the stability of estuarine stratification on different timescale are analyzed using Richardson number and stratification parameter $\frac{\Delta S}{\langle S \rangle}$, where ΔS and $\langle S \rangle$ are salinity difference between the bottom and the surface and vertical averaged salinity respectively.

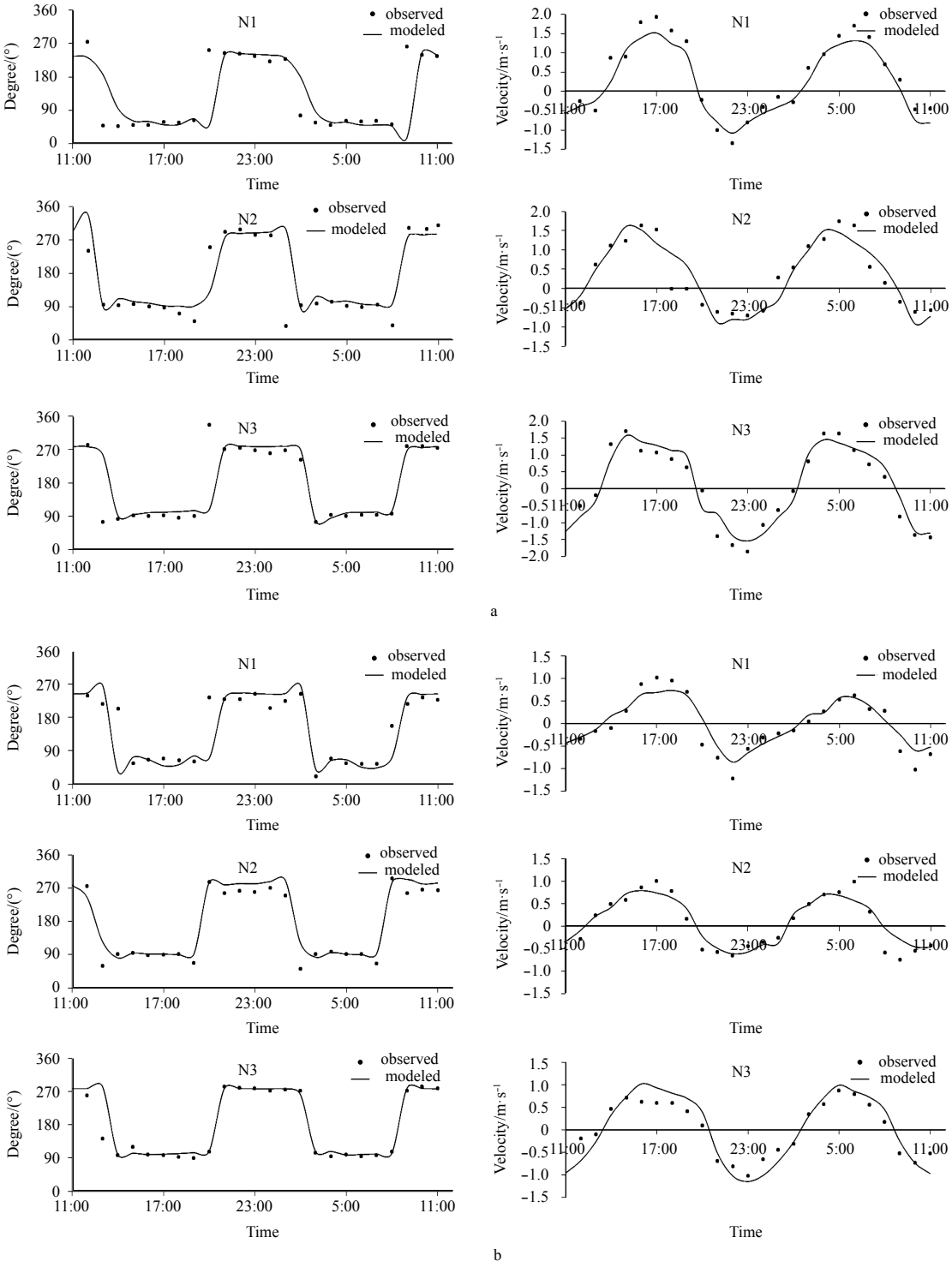

Fig. 5. Comparisons of flow direction and velocity at N1, N2 and N3, respectively. a. Surface and b. bottom.

4.1 *Vertical and temporal variation of salinity*

Figure 7 shows the variations of salinity and velocity at the three locations. The river discharge is 330 m^3/s, while tidal level variation during ebb is 3.9 and 4.8 m during flood. At ND, the stratification is weak at early flood, with salinity difference of about 1.8 from the bottom to surface (Fig. 7a, Hour 6) and depth averaged salinity of 4.3. One hour later, the water column becomes well mixed with salinity of about 5.6. Vertical distribution of velocity is relatively even during flood tide. Maximum depth-averaged velocity is about 1.38 m/s with the difference of about 0.35 m/s from the surface to bottom. At high tidal level, the salinity is nearly 17–20. At the beginning of ebb, significant stratification develops in the upper part, while the middle and lower layer keep well-mixed with salinity of more than 20. The difference of salinity is nearly 7 from surface to bottom. About 5 h later, stratification disappears. During ebb, the velocity exhibits strong vertical shear until the maximum low tidal level. The maximum vertical shear is near middle tidal level with the magnitude of 1 m/s.

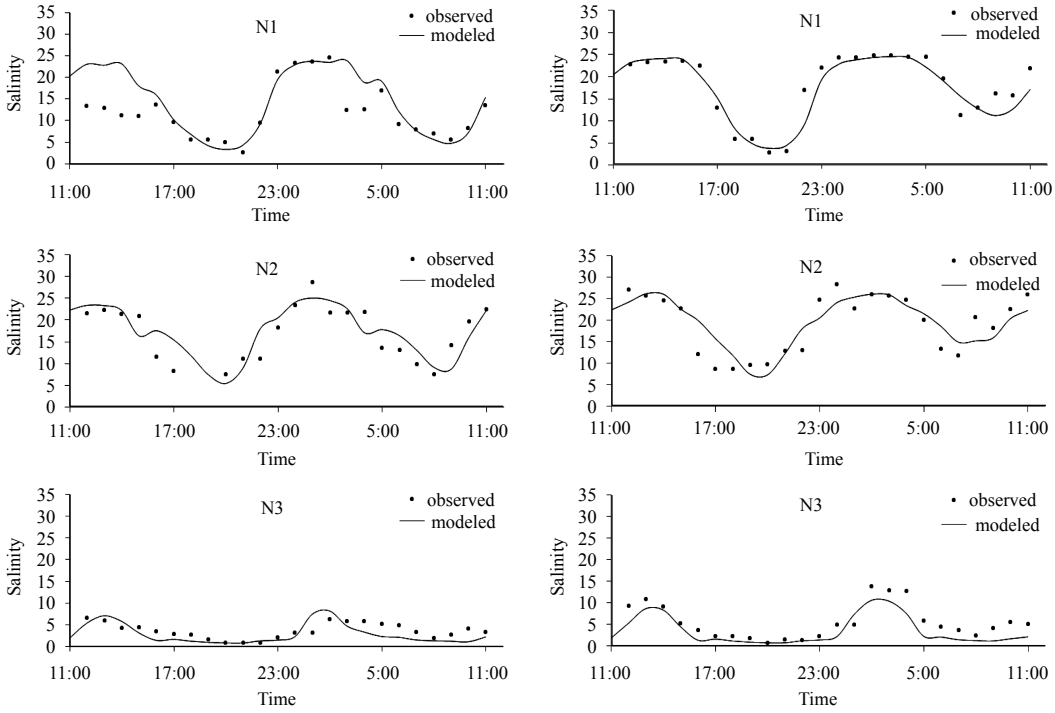

Fig. 6. Comparisons of salinity for surface (left panel) and bottom (right panel) layer at N1, N2 and N3, respectively.

Table 1. Statistics of tidal elevation

	Meiao	Wuniu	Qili	Luxi	Wuxiantou	Nanshan
MAE elevation/m	0.26	0.29	0.24	0.30	0.19	0.22
Skill elevation/m	0.99	0.99	0.99	0.98	0.99	0.99

Table 2. Statistics of tidal velocity and salinity

		N1		N2		N3	
		surface	bottom	surface	bottom	surface	bottom
Velocity/m·s^{-1}	MAE	0.25	0.17	0.22	0.15	0.29	0.22
	Skill	0.97	0.96	0.98	0.96	0.98	0.96
Direction/(°)	MAEA	10.50	16.14	12.73	11.36	7.61	5.37
	Skill	0.91	0.91	0.95	0.96	0.92	0.97
Salinity	MAE	3.38	1.91	2.80	2.89	1.57	1.75
	Skill	0.96	0.80	0.91	0.84	0.82	0.81

At N3, the salinity process shows very similar features to ND. Though it is absolutely fresh of 2–4 during low water, the water column exhibits slight stratification. Salinity difference from the bottom to surface is about 0.7–1.0 (Fig. 7b). Since the water is relatively fresh, the stratification parameter $\frac{\Delta S}{\langle S \rangle}$ is about 0.25. The stratification lasts less than one hour and then the water is well-mixed until high water. The surface velocity of maximum flood is about 1.4 m/s with a difference of 0.3 m/s vertically. At high water, averaged salinity is about 3, which is less than that of ND. During early ebb, the water column stratifies with a vertical salinity difference of about 6.3 h after high tidal level, the water returns to well-mixed.

The upstream NU station (Fig. 7c) reveals different features from those of N3 and ND. Stratification arises immediate after high tidal level, while the water is well-mixed at low level. At low water, the salinity is less than 2 because of downstream transport of fresh water. At high water, the salinity is about 11 at the lower two-thirds of water column and 7–8 at the surface layer with velocity less than 0.2 m/s. When ebb begins, the water becomes stratified for about 3 h and then stays well-mixed until the next

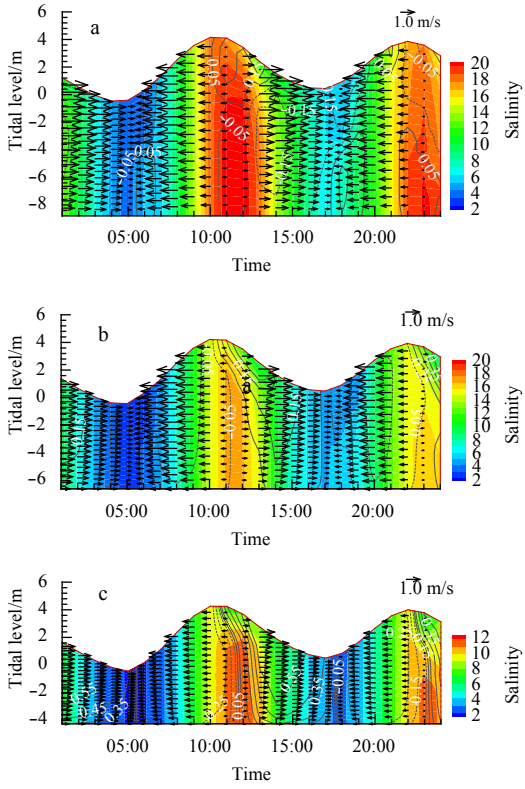

Fig. 7. Evolution of salinity and velocity at ND (a), N3 (b) and NU (c). Arrow represents along-channel velocity and gray lines represent cross-sectional velocity.

highest salinity of 6–7. Vertically-averaged velocity and vertical shear is smaller than that of N3 and ND. Maximum ebb velocity is about 1.1 m/s at surface layer and the maximum difference vertically is about 0.6 m/s. During flood tide, the maximum velocity and vertical shear are about 0.9 and 0.27 m/s, respectively.

According to the previous discussion, the stratification processes in the ORE show different behavior from the common patterns where stratification develops during ebb tide and weakens during flood. This is due to the specific bathymetric and hydrodynamic conditions. Because of the relatively large tidal range and tidal velocity, the tidal excursion is about two times longer than the length of the lower estuary. The upper limit of saltwater moves to and fro and can withdrawal out of the river mouth during low water. Moreover, as the river discharge increases, upper limit of salinity intrusion is pushed downstream and the water in the north branch becomes quite fresh.

4.2 *Intertidal variations of stratification*

Estuarine classification is a key component in estuarine studies. Several methods have been proposed in the past several decades (Dyer, 1997; Valle-Levinson, 2010), however, most of them are statistically averaged. The classification based on temporal stratification and mixing of intratidal or spring-neap scales are not widely concerned in the ORE. Therefore, two indices are discussed to elucidate the intertidal variation of salinity stratification here.

Prandle (1985) defined a stratification number S_t to evaluate the estuarine mixing which is written as

$$S_t = \frac{0.85kU_0L}{(\Delta\rho/\rho)gh^2U_f}, \tag{6}$$

where k is friction coefficient, U_0 is amplitude of the tidal currents, h is water depth, U_f is river flow, g is gravity acceleration, $\Delta\rho$ and ρ are the density difference between the fresh and sea water density.

Prandle (1985) gave thresholds of S_t according to estuarine mixing conditions. The values of S_t were also compared with $\frac{\Delta S}{\langle S\rangle} = 4S_t^{-0.55}$ and presented thresholds as: $\frac{\Delta S}{\langle S\rangle} < 0.15$ for well-mixed, $\frac{\Delta S}{\langle S\rangle} > 0.32$ for straitified, $0.15 < \frac{\Delta S}{\langle S\rangle} < 0.32$ for partially mixed. It should be noted that in Hansen and Rattray's stratification-circulation diagram, $\frac{\Delta S}{\langle S\rangle} = 0.1$ is the threshold between stratified and mixed conditions.

Fischer (1972) introduced an estuarine Richardson number (Ri_e) representing the ratio of gain of potential energy due to freshwater discharge to the mixing power of the tidal currents, which is defined as

$$Ri_e = \frac{\Delta\rho}{\rho}\frac{gQ}{WU_t^3}, \tag{7}$$

where Q is freshwater discharge, W is estuary width, U_t is root-mean-square tidal current. For Ri_e<0.08 well-mixed, Ri_e>0.8 straitified, 0.08<Ri_e<0.8 partially stratified.

Figure 8 shows the evolution of river discharge, daily-mean

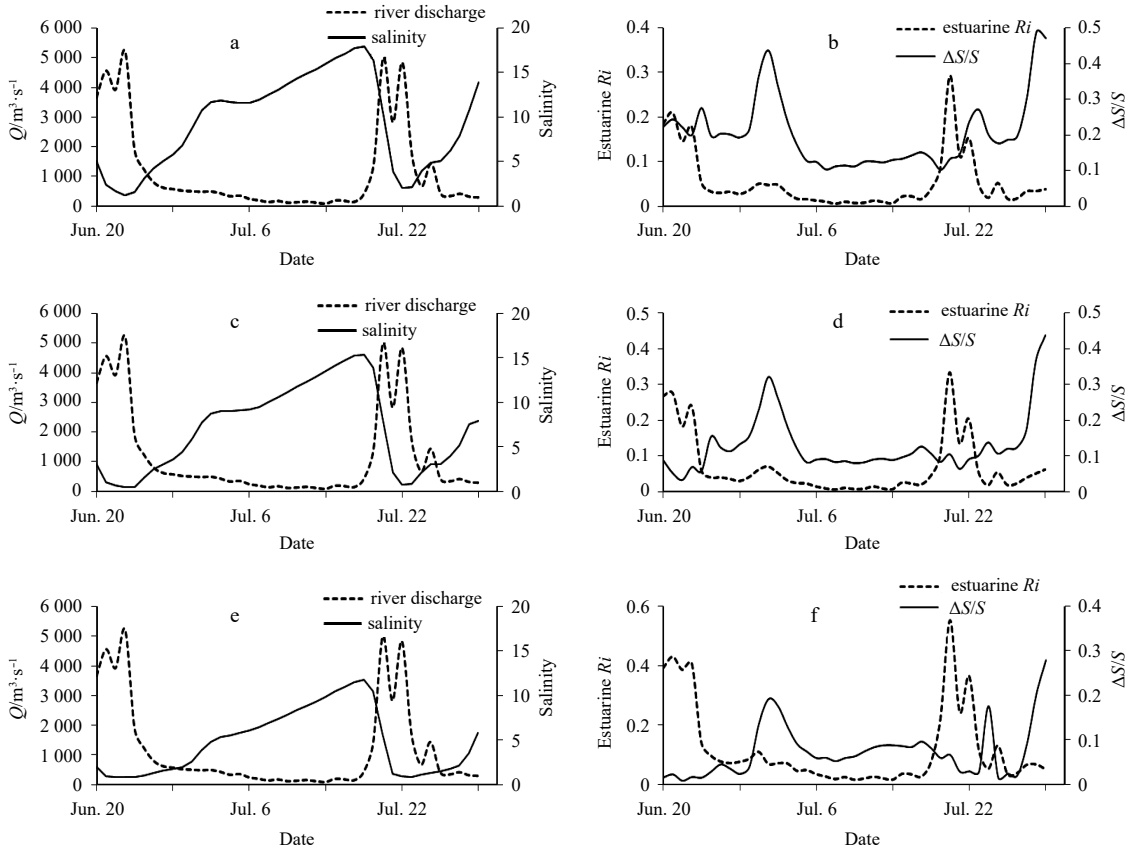

Fig. 8. River discharge and daily-mean salinity (left panel); Estuarine Richard number and stratification parameter (right panel) at ND, N3 and NU, respectively. The above two are for ND, middle for N3 and bottom for NU, and all date are for the year 2005.

vertical averaged salinity, Ri_e and $\frac{\Delta S}{\langle S\rangle}$ during the period from June 20 to July 30 at the sample points. Apparently, the trends are similar except for their different values. It can be seen that the mean salinity increases persistently from June 23 when a freshet existed and exceeded 5 000 m³/s to the next freshet on July 20. During this period, the river discharge decreases slowly. The minimum discharge is about 120 m³/s and the maximum salinity decreases spatially from the river mouth (ND) of 18 to upstream (NU) of 11.6. During freshets, the salinities are below 2 indicating that all the lower estuarine segments are substantially fresh. The salinity in the estuary seems to be not connected closely to tide but changes almost simultaneously with river discharge. According to the thresholds, both Ri_e and $\frac{\Delta S}{\langle S\rangle}$ of NU indicate that the upper segment of the north branch is well-mixed permanently except for two short periods. Meanwhile at the river mouth (ND) as shown in Fig. 8, the water appears to be partially mixed ($0.15 < \frac{\Delta S}{\langle S\rangle} < 0.32$) and short periods of well-mixed ($\frac{\Delta S}{\langle S\rangle} < 0.15$) and stratified ($\frac{\Delta S}{\langle S\rangle} > 0.32$).

As a result, the ORE exhibits periodic stratification on intertidal timescales. According to Eq. (7), Ri_e varies in pace with river discharge expectedly. Meanwhile, the stratification represented by $\frac{\Delta S}{\langle S\rangle}$ seems to lag river discharge for several days in freshet. The $\frac{\Delta S}{\langle S\rangle}$ is a direct expression of water stratification while Ri_e includes river discharge and is sensitive to it. The lag is not due to adjustment of the ORE to the freshet but the rapid loss of salt in the river volume. Salinity in the ORE reacts quickly to freshets. During freshet periods, river drainage keeps the water fresh in the north branch. At the same time, the stratification parameter $\frac{\Delta S}{\langle S\rangle}$ increases inconspicuously, which means that stratification indicated by Ri_e dose not emerge. This indicates that since the ORE is considerably short, it may be of different regimes proposed by Hansen and Rattray (1965) during different riverine conditions. $\frac{\Delta\rho}{\rho} = 0.025$ is adopted when calculating the Eq. (7). However, it is worthy to be noticed that the $\Delta\rho$ is defined as salinity difference between river water and ocean water (Fischer, 1972). The ORE might essentially include the areas outside the river mouth. The complex topography and hydrodynamic process make it substantially difficult to obtain precise evaluation of $\frac{\Delta\rho}{\rho}$. Thus the application of Ri_e calculated with Eq. (7) ought to be with caution in the ORE.

Figure 9 shows the variations of stratification parameter against river discharge and tidal range at NU, N3 and ND. The stratification is represented by $\frac{\Delta S}{\langle S\rangle}$, which is calculated hourly and then averaged daily. The NU is well-mixed when river dis-

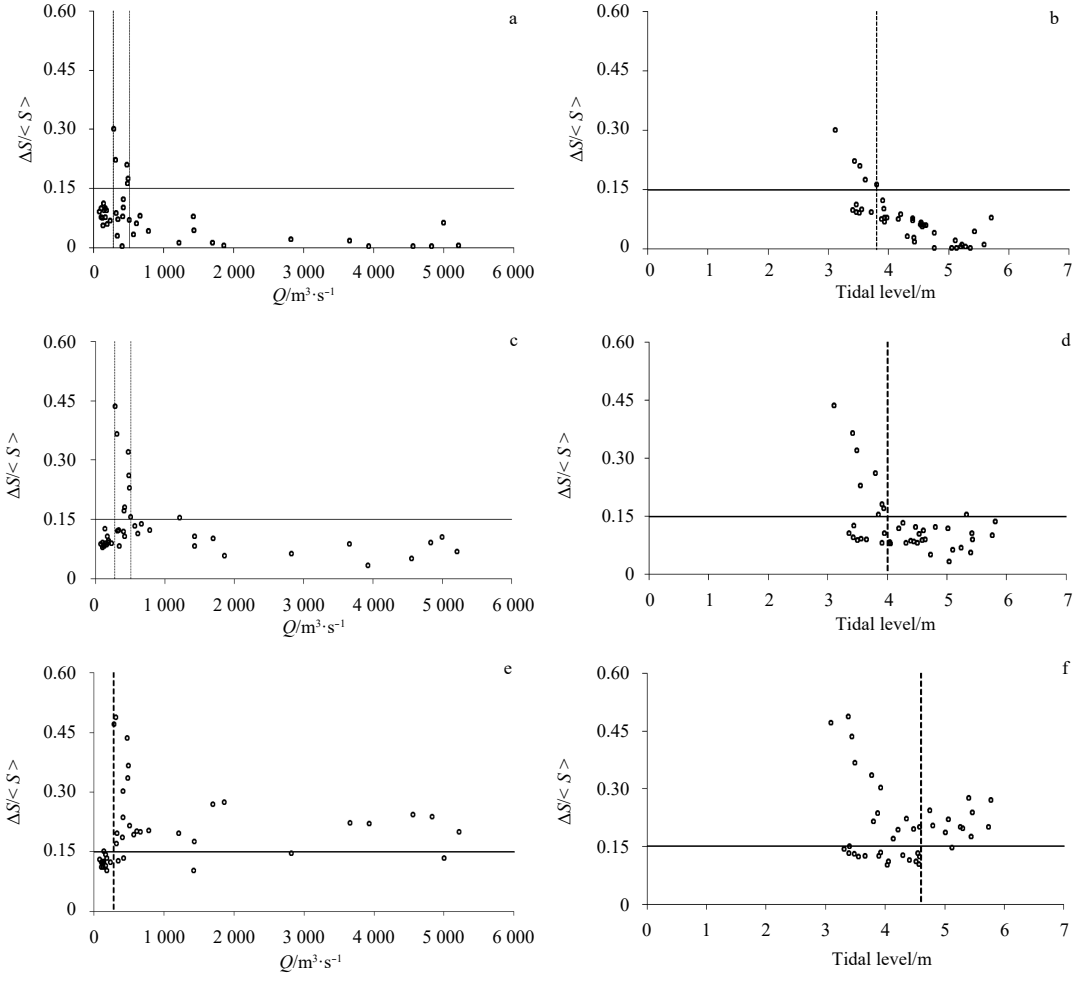

Fig. 9. Stratification parameter against river discharge (a, c, e) and tidal level (b, d, f) at NU, N3 and ND.

charge is less than 280 m^3/s or exceeds 510 m^3/s or tidal range is greater than 3.8 m. It also shows that in only a few days the stratification parameter exceeds 0.15 indicating partial mixing. At N3, the water is well-mixed while the river discharge is larger than 510 m^3/s or less than 280 m^3/s. Meanwhile there exists sustainable well-mixed conditions when the tidal range exceeds 4 m. For ND at the river mouth, the water is stratified when river discharge is larger than 280 m^3/s or tidal range exceeds 4.6 m. On the other hand, while river runoff is less than 280 m^3/s, the ND is well-mixed. Meanwhile, the ND may be stratified or well-mixed depending on river discharge as the tidal range decreases below the 4.6 m. Under conditions of small tidal range, the N3 and ND also exhibit high stratifications for $\frac{\Delta S}{\langle S \rangle} > 0.32$.

For further investigation, regressions of $\frac{\Delta S}{\langle S \rangle}$ against tidal range and river change are conducted basing on the data under stratified conditions. Results are shown in Table 3. It can be seen that there are acceptable linear relationship between $\frac{\Delta S}{\langle S \rangle}$ and tidal range and river discharge. The stratification parameters can be well calculated using the regression equations at N3 and NU, but maybe contain relatively larger deviations at ND than N3 and NU. The linear regression shows that estuarine stratification is negatively related to river discharge, and in Fig. 8 the Ri_e increases dramatically while $\frac{\Delta S}{\langle S \rangle}$ decreases slightly. This result seems to contradict common sense. This is because that from July 20 to July 22, the river discharge increases greatly and leads to a simultaneous increment in Ri_e. However, as the river discharge increases, upper limit of salinity intrusion is pushed downstream and the water becomes quite fresh. This also means that Ri_e might not be a proper parameter in the Oujing Estuary when only the segments upstream the river mouth are considered.

Table 3. Regression of stratification parameter against tidal range and river discharge

Sample point	Regression equation	$\lvert R \rvert$	$R_{0.05}$
NU	$Sp = 0.904\,2 - 0.191\,2 \times Tr - 0.000\,051 \times Q$	0.984	0.755
N3	$Sp = 1.378\,5 - 0.227\,4 \times Tr - 0.000\,252 \times Q$	0.951	0.878
ND	$Sp = 0.558\,6 - 0.069\,5 \times Tr + 0.000\,61 \times Q$	0.565	0.404

Note: Sp is stratification parameter $\Delta S / \langle S \rangle$, T_r is tidal range.

4.3 *Stratification dynamics*

The dynamic equation of the potential energy anomaly (PEA) for analyzing stratification proposed by Burchard and Hofmeister (2008) has been used in estuarine stratification research. We apply this equation in the ORE for quantitatively analysis of the relevant terms from model results to discuss generation and destruction of stratification. The period of July 4–5 is chosen for analysis for its medium tidal range and river discharge.

Figures 10a, c and e show the temporal gradient of PEA and the sum of all right-hand side terms in Eq. (1). As it is shown, the acceptable agreements indicate that the fundamental trench of PEA evolution can be composed by the modeled individual terms. At ND, there are distinct increments during flood tide (Hours 6 and 17) and ebb tide (Hour 13). At N3, peaks similar to ND also exist. However, the NU exhibits different features from those of N3 and ND. There is almost no change during flood tide while there are distinct increments during early ebb and followed by immediate decrease. These features coincide with what revealed in Figs 7a and b.

From Fig. 10b, it can be seen that the increase during early flood are caused mainly by longitudinal advection and lateral depth-mean straining near river mouth. During the transition of low water, clear lateral circulation develops at the end of ebb, which causes important lateral shear. Meanwhile, during low wa-

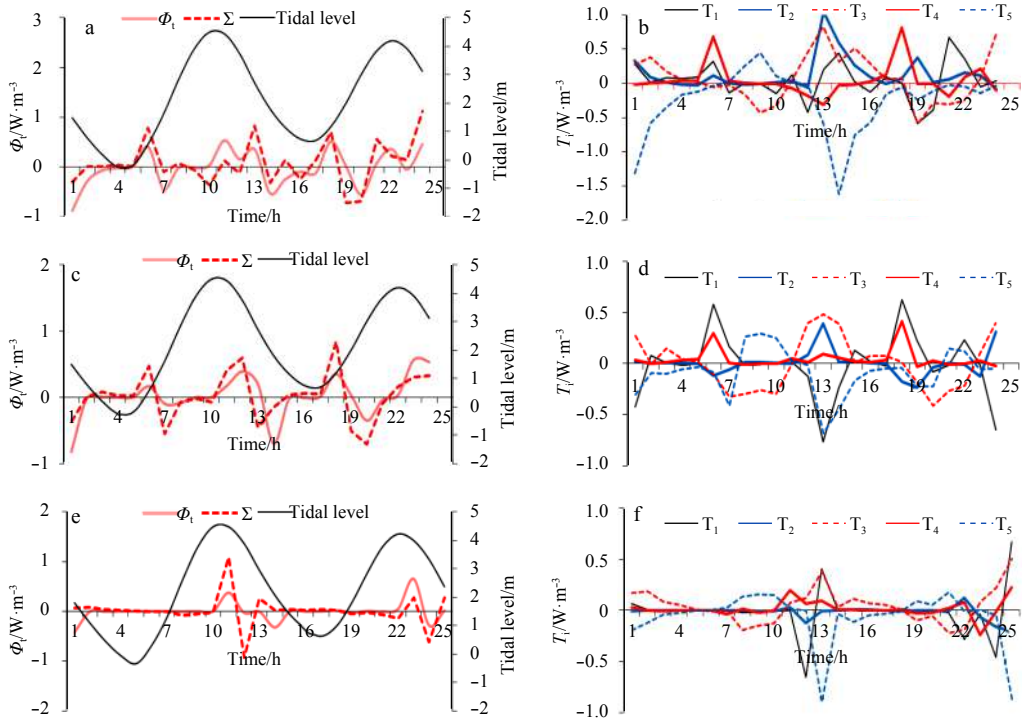

Fig. 10. Temporal variation of terms in Eq. (1) at ND, N3 and NU (the above two are for ND, middle for N3 and bottom for NU). Φ_t is temporal gradient of PEA, $\sum$ means sum of the RHS terms. T_1, T_2, T_3, T_4 and T_5 denote the first five terms on the right side of Eq. (1).

ter, the water stratification is stronger in the downstream areas (Fig. 7a). While during early ebb, the increases of stratification are primarily introduced by the lateral advection and longitude depth-mean straining. After then, the strong mixing due to enhanced tidal current decreases the PEA. Longitudinal tidal advection and lateral current shear contribute to the increase of PEA during early flood tide in the middle part (N3), while tidal straining in the main direction and vertical tidal mixing cause the decrease of PEA. During early ebb tide, the increases of PEA are mainly due to longitudinal tidal depth-mean strain and lateral advection. As the ebb continues, upstream water of less salinity reaches and velocity increases significantly. As a result, longitudinal advection and vertical turbulent mixing become strong and weaken the stratification. At NU, during early ebb tide there is no predominant effect that contributes to the enhanced stratifications (Fig. 10f). Residual mechanisms might be the dominant factors. However, near the upstream conjunction, there is a deep hollow and a dike that is submerged and exposed on different tidal stages, and water is relatively shallower and fresher in this area. These complex factors might lead to substantially complicit stratification processes. After the brief stratification, PEA decreases since the well-mixed fresher water reaches. This is revealed in Fig. 10f that longitudinal advection plays a dominant role in the following stratification attenuation.

5 Conclusions

A 3-D numerical simulation using FVCOM is conducted to overcome the deficiencies of former understandings on stratification and mixing in the ORE which has large tidal range, drastic variation of runoff and many islands outside the estuary. The intratidal and intertidal variations of salinity stratification are investigated according to the model results. The dynamic equation of potential energy anomaly is adopted to evaluate relevant terms and analyze the stratification mechanism.

Periodic stratification exists in the north branch under ordinary hydrodynamic conditions even for large tidal range. At early ebb and flood, the lower estuary appears to be partially stratified while well-mixed in other tidal stages. Upper limit of salinity intrusion moves to and fro and can withdrawal out of the river mouth during low water due to the short length of the ORE. The upper limit of salinity intrusion is pushed downstream and the water becomes greatly fresh under large river discharge. This causes distinct characteristics of the stratification evolution at different locations and different hydrodynamic conditions.

The enhancement of stratification during early flood is due to longitudinal advection and lateral velocity shear, while turbulent mixing and longitudinal tidal straining are the main factors of stratification attenuation. In the upper segment of the north branch, there is no stratification during low tide. Stratification only develops during early ebb tide due to interactions between vertical variations of velocity and density gradients. Then, stratification disappears due to the transport of fresh river water.

The north branch of the ORE exhibits well-mixed conditions when the tidal range exceed 3.8 m, 4.0 m and 4.6 m at NU, N3 and ND, respectively. Meanwhile, when river discharge is less than 280 m^3/s or greater than 510 m^3/s, the estuary is also well-mixed sustainably at upper segments of the north branch. Near the river mouth, river discharge of 280 m^3/s is a rough critical value that separate well-mixed and stratified states. A regression equation is obtained to express the relationship between the estuarine stratification and the riverine discharge and tidal range. The linear regression shows that estuarine stratification is negatively related to river discharge that conflicts common sense. This is because that the head of saltwater intrusion moves the north branch and the water becomes quite fresh and of minor vertical density variation when riverine discharge increases. It should be noticed that the critical values of tidal range and river discharge evaluating stratification state is just based on this simulation. More precise values need to be investigated by further field and experimental measurements.

Acknowledgements

We thank two anonymous reviewers for their constructive comments. We also thank Khan Ziad and Lombe Mwelwa for reading the manuscript.

References

Burchard H, Baumert H. 1998. The formation of estuarine turbidity maxima due to density effects in the salt wedge. A hydrodynamic process study. Journal of Physical Oceanography, 28(2): 309–321, doi: 10.1175/1520-0485(1998)028<0309:TFOETM>2.0.CO;2

Burchard H, Hofmeister R. 2008. A dynamic equation for the potential energy anomaly for analysing mixing and stratification in estuaries and coastal seas. Estuarine, Coastal and Shelf Science, 77(4): 679–687, doi: 10.1016/j.ecss.2007.10.025

Chant R J, Stoner A W. 2001. Particle trapping in a stratified flood-dominated estuary. Journal of Marine Research, 59(1): 29–51, doi: 10.1357/002224001321237353

Chen Changsheng, Liu Hedong, Beardsley R C. 2003. An unstructured grid, finite-volume, three-dimensional, primitive equations ocean model: application to coastal ocean and estuaries. Journal of Atmospheric and Oceanic Technology, 20(1): 159–186, doi: 10.1175/1520-0426(2003)020<0159:AUGFVT>2.0.CO;2

Cheng Peng, Wilson R E, Chant R J, et al. 2009. Modeling influence of stratification on lateral circulation in a stratified Estuary. Journal of Physical Oceanography, 39(9): 2324–2337, doi: 10.1175/2009JPO4157.1

de Boer G J, Pietrzak J D, Winterwerp J C. 2008. Using the potential energy anomaly equation to investigate tidal straining and advection of stratification in a region of freshwater influence. Ocean Modelling, 22(1–2): 1–11, doi: 10.1016/j.ocemod.2007.12.003

de Vries J J, Ridderinkhof H, Maas L R M, et al. 2015. Intra- and intertidal variability of the vertical current structure in the Marsdiep basin. Continental Shelf Research, 93: 39–57, doi: 10.1016/j.csr.2014.12.002

Dyer K R. 1997. Estuaries: A Physical Introduction. 2nd ed. New York: John Wiley & Sons

Fischer H B. 1972. Mass transport mechanisms in partially stratified estuaries. Journal of Fluid Mechanics, 53(4): 671–687, doi: 10.1017/S0022112072000412

Flores R P, Rijnsburger S, Horner-Devine A R, et al. 2017. The impact of storms and stratification on sediment transport in the Rhine region of freshwater influence. Journal of Geophysical Research, 122(5): 4456–4477

Geyer W R, MacCready P. 2014. The estuarine circulation. Annual Review of Fluid Mechanics, 46: 175–197, doi: 10.1146/annurev-fluid-010313-141302

Hansen D V, Rattray Jr M. 1965. Gravitational circulation in straits and estuaries. Journal of Marine Research, 23: 104–122

Li Ming, Zhong Liejun, Boicourt W C. 2005. Simulations of Chesapeake Bay estuary: Sensitivity to turbulence mixing parameterizations and comparison with observations. Journal of Geophysical Research, 110(C12): C12004, doi: 10.1029/2004JC002585

Lin Weibo, Wang Yigang, Ruan Xiaohong, et al. 2012. Modeling residual circulation and stratification in Oujiang River Estuary. China Ocean Engineering, 26(2): 351–362, doi: 10.1007/s13344-012-0027-z

MacCready P, Geyer W R. 2010. Advances in estuarine physics. Annual Review of Marine Science, 2: 35–58, doi: 10.1146/annurev-

marine-120308-081015

Marques W C, Fernandes E H L, Rocha L A O. 2011. Straining and advection contributions to the mixing process in the Patos Lagoon estuary, Brazil. Journal of Geophysical Research, 116(C3): C03016

Mayer D G and Butler D G, 1993. Statistical validation. Ecological Modelling, 68: 21–32, doi: 10.1016/0304-3800(93)90105-2

Monismith S G, Burau J R, Stacey M T. 1996. Stratification dynamics and gravitational circulation in northern San Francisco Bay. In: Hollibaugh T, ed. San Francisco Bay: The Ecosystem. Washington, DC: American Association for the Advancement of Science Pacific Division

Prandle D. 1985. On salinity regimes and the vertical structure of residual flows in narrow tidal estuaries. Estuarine, Coastal and Shelf Science, 20(5): 615–635, doi: 10.1016/0272-7714(85)90111-8

Pu Xiang, Shi J Z, Hu Guodong, et al. 2015. Circulation and mixing along the North Passage in the Changjiang River estuary, China. Journal of Marine Systems, 148: 213–235, doi: 10.1016/j.jmarsys.2015.03.009

Ralston D K, Geyer W R, Traykovski P A, et al. 2013. Effects of estuarine and fluvial processes on sediment transport over deltaic tidal flats. Continental Shelf Research, 60(Suppl): S40–S57

Shanghai Marine Engineering Survey and Design Institute (SMESDI). 2005. Field measurements of Hydrology and sediment in Wenzhou Oujiang Reclamation project -Technical Report

Sharples J, Simpson J H, Brubaker J M. 1994. Observations and modelling of periodic stratification in the Upper York River Estuary, Virginia. Estuarine, Coastal and Shelf Science, 38(3): 301–312, doi: 10.1006/ecss.1994.1021

Simpson J H, Bowers D. 1981. Models of stratification and frontal movement in shelf seas. Deep Sea Research Part A. Oceanographic Research Papers, 28(7): 727–738

Simpson J H, Brown J, Matthews J, et al. 1990. Tidal straining, density currents, and stirring in the control of estuarine stratification. Estuaries, 13(2): 125–132, doi: 10.2307/1351581

Simpson J H, Sharples J, Rippeth T P. 1991. A prescriptive model of stratification induced by freshwater runoff. Estuarine, Coastal and Shelf Science, 33(1): 23–35, doi: 10.1016/0272-7714(91)90068-M

Valle-Levinson A. 2010. Definition and classification of estuaries. In: Valle-Levinson A, ed. Contemporary Issues in Estuarine Physics. Cambridge: Cambridge University Press, 1–11

Wang Shunzhong, Li Haolin. 2001. Model study of Yangfushan reclamation project in Oujiang River. Ocean Engineering (in Chinese), 19(1): 51–58

Wang Liuyang, Shen Yongming. 2014. Study on hydrodynamic environment of land-making project at Wenzhou shoal. Chinese Journal of Hydrodynamics (in Chinese), 29A(1): 67–75

Warner J C, Sherwood C R, Arango H G, et al. 2005. Performance of four turbulence closure models implemented using a generic length scale method. Ocean Modelling, 8(1–2): 81–113, doi: 10.1016/j.ocemod.2003.12.003

Willmott C J. 1981. On the validation of models. Physical Geography, 2(2): 184–194, doi: 10.1080/02723646.1981.10642213

Xu Ting, You Xueyi. 2016. Effects of large-scale embankments on the hydrodynamics and salinity in the Oujiang River Estuary, China. Journal of Marine Science and Technology, 22(1): 71–84, doi: 10.1007/s00773-016-0394-x

Xu Ting, You Xueyi. 2017. Numerical simulation of suspended sediment concentration by 3D coupled wave-current model in the Oujiang River Estuary, China. Continental Shelf Research, 137: 13–24, doi: 10.1016/j.csr.2017.01.021